Air Permeability of Undisturbed Soils

Noboru NAGATA

1. Introduction

The Soil plays a very important role in storing up water and nutrients and supplying them to plants. In addition, the soil also contributes to plant growth through exchange of gases between the air and it. The exchange is mainly due to the increase of concentration of carbonic acid gas in soil accompanied with decomposition of organic matters by soil microorganisms.

The researcher who studied firstly gas exchange in soil was Buckingham. He performed the study on the basis of the Fick's law and a theory of motion of molecules. Following him, many researchers (e.g. Penman, and Taylor) have studied this problem. As a result, relationships between diffusion constant and amont of air-filled pores in soil have been considerably made clear. On the other hand, many researchers (e.g. Zunker, King, Slicher, Tamachi, Morishima and Kinoshita) have performed researches about air permeability of soil from the viewpoint of air flow owing to difference of air pressures, regarding soil as a porous medium. However, some problems related to air permeability of soil have been remained.

The object of this study is to clarify relationships between air permeability and pore structure in several soils and those between air and water permeabilities in the soils from the standpoint of air flow induced by difference of air pressures. In the experiments, undisturbed samples of the soils were mainly used. In addition, packed soil samples were also used as supplement.

2. Experimental Methods and Materials

2-1 Measurement of air permeability

Measurements of air permeability are divided into two main classes; measuring methods in field and those in laboratory[6]. In this study, the following measuring method was used: Fig. 1 shows the apparatus measuring aie permeability of soil. A in Fig. 1 is a metal cylinder in which a soil sample exists. The cylinder is inserted into a thick rubber plate, B, in order to keep the apparatus airtight. F is a tank to prevent a sudden air pressure change in a glass vessel, C, when a vacuum pump or a sucker connected with the pipe on the lefthand is working. The volume of the tank is about 10^5 cm^3. According to setting up the tank, the change of air pressure in C can be regarded to be negligible. The difference in air pressure between the both sides of the sample can be read to 0.1 mm (in water column). In addition, the amount of air flow is measured by a gas flow meter, D, and the temperature in C is also measured.

2-2 Investigation of validity of the Darcy law

When the Darcy law is applied to air flow through a porous medium, the following equation is obtained

$$v = -k_a \frac{\partial P}{\partial x} \tag{1}$$

where v is the average velocity, k_a is the air conductivity, x is the coordinate taken along the direction of

Received October 30, 1987

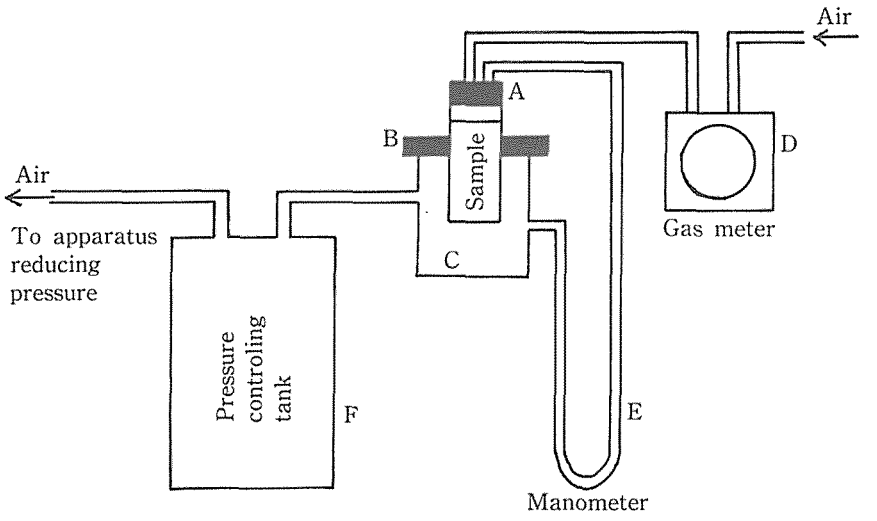

Fig. 1 A shcematic representation of apparatus mesuring air coductivity.

the air flow, and P is the air pressure. Assuming that 1) $\rho_a v$ (ρ_a: dinsity of the air) and $v/(\frac{\partial P}{\partial x})$ are constant and 2) the change of air flow is done under an isothermal condition, Eq.(1) is transformed into Eq.(2).

$$v = k_a \frac{\overline{P}}{P} \frac{(P_1 - P_2)}{L} \tag{2}$$

where $P=\rho_a RT$ (R: gas constant, T: temperature), $\overline{P}=\overline{\rho}_a RT$, ($\overline{\rho}_a$: the average density of the air), P_1 and P_2 are the air pressures at the inlet and outlet of the sample, respectively, and L is the length of the sample.

Supposing that the sectional area of the sample is A and the mass of outflowing air per unit time is M, Eq.(2) becomes

$$M = \rho_a v A = A\rho_a k_a \frac{(P_1 - P_2)}{L} \tag{3}$$

Writing q for the average volume of outflowing air per unit time and ΔP for $(P_1 - P_2)$, the following equation is obtained

$$q = Ak_a \frac{\Delta P}{L} \tag{4}$$

Consequently, k_a can be obtained by knowing q, A, L and ΔP.

According to Lindquist[4], the Darcy law is applicable for a flow whose Reynolds number, Re, is smaller than 4. Since a sand with a diameter of 1~2 mm is commposed of the largest particles among the materials used here, Re of air flow through it is considered to be the largest. The Re for the sand was 3.7 even if the maximum value of air velocity measured in the experiments for the sand was used for the calculation of the Re. This means that the Darcy law is valid under the experimental conditions in this study. In additon, after confirming that, in each measurement, a relationship between $\Delta h/L$ and q/A was linear as a function of Δh, the k_a was obtained by measuring the gradient of the line. An example of the results is shown in Fig. 2.

The relationship between air conductivity, k_a, and air content in a soil sample was measured by the following procedure: 1) Firstly, the soil sample is saturated with water. 2) Then, the water is dried

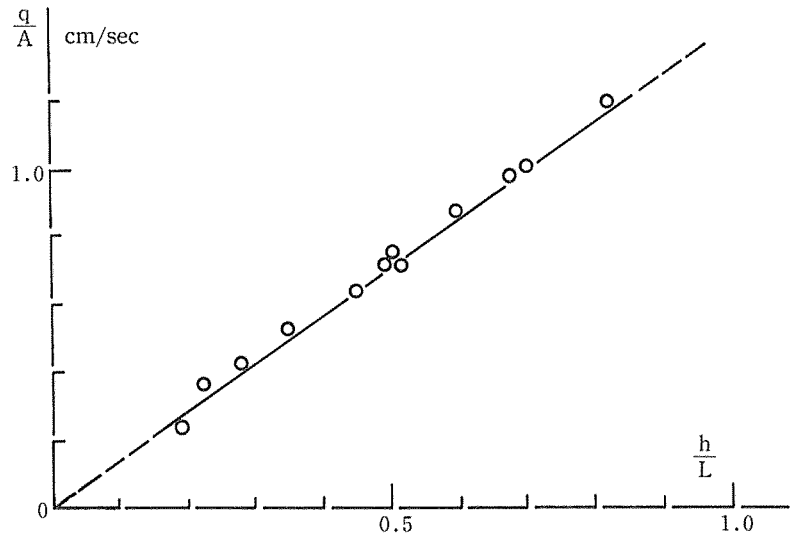

Fig. 2 q/A～h/L relationship.

slowly (the air volume is slowly increased). 3) The air conductivities are measured at given air volumes in the process of drying.

2–3 Drying apparatus for soil sample

The drying was performed using an apparatus shown in Fig. 3. The concentration of H_2SO_4 solution indicated in the figure is around 55%, and its equilibrium relative humidity is about 30%. Air is circulated from the right side of the sample to the left side by a pump. That is, 1) air passes through the H_2SO_4 solution at the right side as bubles, 2) as a result, the relative humidity of the air is lowered, 3)

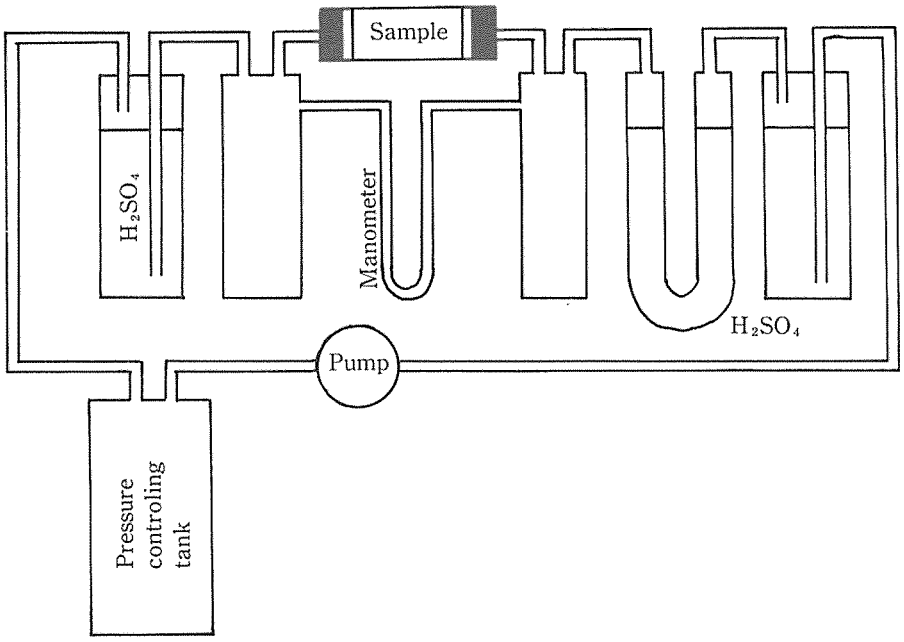

Fig. 3 A schematic representation of apparatus drying sample.

then, the air goes through the sample, 4) consequently, the sample is dried up, 5) the air wetted by going through the sample again passes through the H_2SO_4 solution at the left side. The degree of drying of the sample with time is checked by measuring the weight of the sample at regular intervals. In addition, the situation of the sample is inverted sometimes to ensure uniform drying in the sample. As a result, distributions of water contents in soil samples were considerably uniform as shown in Table 1.

2-4 Materials

Undisturbed samples were taken in such a way that 1) holding a metal cylinder with a inside diameter of 4.8 cm and a length of 15 cm vertically, the cylinder is inserted gently into a soil layer with care unitil the soil surface just emerges from the cylinder and 2) the cylinder is dug out.

Table 2 shows the soil types, the soil textures, the average water contents at the sampling times, $\overline{w}$, and the average air conductivities, $\overline{k_a}$, of respective samples used here. In addition, $\overline{k_a}$ is an average of values estimated at 20°C by correcting results measured.

Table 1. Examples of distributions of water content in samples.

Position of sample	Sand	Loam	Clay
Part of one third from one end	10.5 %	13.5 %	20.1 %
Part of one third around middle section	11.3	16.0	25.1
Part of one third from another end	10.8	14.0	18.7
Total	11.0	14.7	22.0

Table 2. Physical properties of undisturbed samples at sampling time.

Kinds of soil	Soil layer		Sampling depth	Soil texture	$\overline{w}$	$\overline{k_a}$
Volcanic ash soils	Nohdai	I	0~ 10 cm	Silty loam	63 %	1.1 cm/sec
		II	30~ 40	Silty clay loam	71	0.73
		III	43~ 53	Silty clay	104	3.8
		IV	80~ 90	Silty clay	138	2.1
		V	140~150	Silty clay loam	128	3.0
	Udai	I	15~ 25	Clay loam	98	0.37
		II	100~110	Silty clay	125	1.4
		III	150~160	Silty clay	131	0.07
		IV	180~190	Clay loam	110	9.3
		V	240~250	Sandy loam	151	0.40
		VI	300~310	Silty loam	113	0.70
Non-volcanic ash soils	Miedai		15~ 25	Sandy loam	12	3.6
	Tsuruoka	II	40~ 50	Silty clay	76	0.80
		III	65~ 75	Silty clay	67	3.2
	Shizudai	I	5~ 15	Clay loam	30	2.0
		II	40~ 50	Clay loam	30	1.7
		III	80~ 90	Clay loam	28	0.21
	Nobono	II	40~ 50	Clay loam	72	2.1
		III	65~ 75	Clay	40	0.37

3. Air conductivities and air-filled porosities of undisturbed samples at the sampling times

Generally, it has been considered that the magnitude of air conductivity in a soil greatly depends on the air volume in it. The average values of k_a and air-filled porosity, P_a (ratio of the air volume to the total volume) of undisturbed different soil samples at the sampling times are shown in Fig. 4. It can be read from the figure that any relationship is not found between k_a and P_a in the different soils. In other words, the air conductivity is defined not only by the air content, but by the spatial arrangement of air-filled pores. That is, there exist isolated air-filled pores which do not take part in air movement. Fig. 5 shows a schematic representation of soil pores by Rode[3]. The air in pore (a) shown in the figure is not connected with that in the neighbouring pores because the paths existing between pore (a) and the neighbouring pores are all blockaded by bond water (water strongly combined by a soil particle). The air in pore (a) is able to be continuous to that in the neighbouring pore only after the bond water blockading the path between the two pores evaporates by drying.

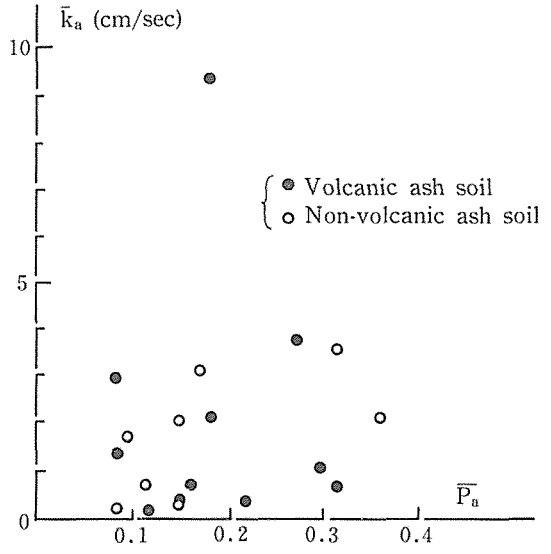

Fig. 4 Relationship between $\overline{k_a}$ and $\overline{P_a}$ at sampling time.

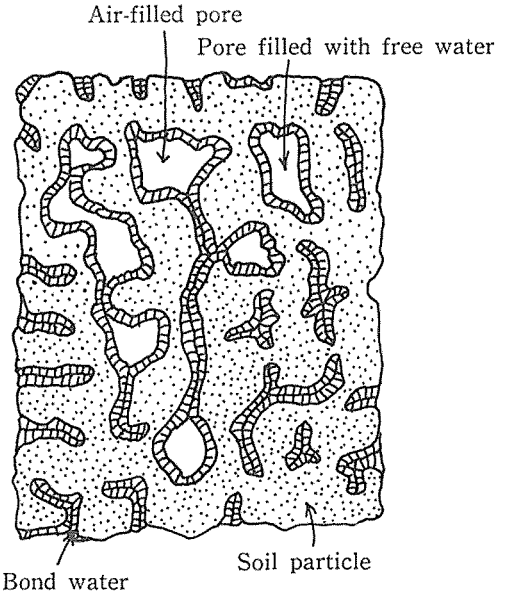

Fig. 5 A schematic representation of soil pores (After Rode).

4. Differential air conductivity

Differential air conductivity is defined by $\Delta k_a/\Delta P_a$ where Δk_a is the increment of air conductivity, k_a, corresponding to an increment of P_a (air-filled porosity), ΔP_a, at a given P_a.

Relationships between log k_a and P_a in the respective undisturbed soil sampls are shown in Fig. 6. These values were obtained using the apparatus described in 2-3. A fact that can be read easily from the figure is: Relationships between log k_a and P_a in all the soils used are expressed by the following experimental equation.

$$\log k_a = \alpha \cdot P_a + \beta \tag{5}$$

where α and β are constants. Of course, for a soil in which the log $k_a \sim P_a$ relationship is represented by two half lines with different gradients from each other, there exist two sets of α and β corresponding to the respective half lines. In many undisturbed soil samples, gaps were formed between soil sample and

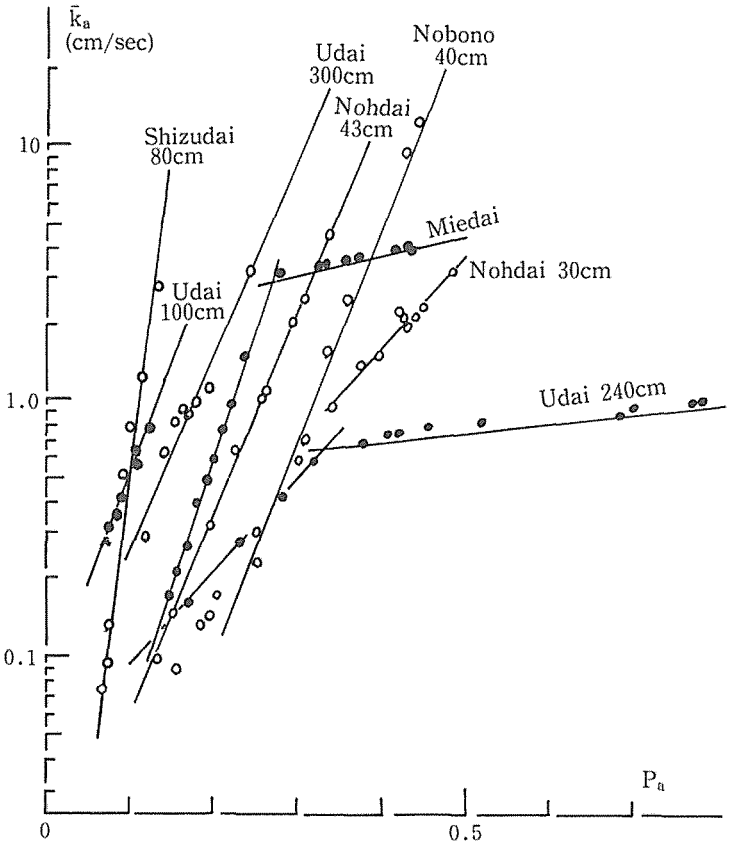

Fig. 6 Relationships between k_a and P_a for undisturbed samples.

wall of sampler in the processes of drying because of shrinkage accompanied to the processes. As a result, the measurements of k_a became impossible. Consequently, the log $k_a \sim P_a$ relationships which are represented by two half lines were recognized only for the soils in which the gaps were difficult to be formed. These soils are Nohdai-30 cm, Udai-240 cm and Miedai as shown in Fig. 6. Buckingham and Penman have also found that linear relationships existed between logarithm of diffusion coefficient of carbonic acid gas and effective air volume in soils.

Differentiating k_a with respect to P_a, the following equation is obtained

$$\frac{\Delta k_a}{\Delta P_a} \fallingdotseq \frac{dk_a}{dP_a} = 2.30\alpha k_a \tag{6}$$

The values of differential air conductivities of the soil samples at P_a=0.2 are shown in Table 3. The reasons why 0.2 is taken as a value of P_a are: 1) The air permeability at $P_a \approx 0.2$ in most of soils plays an important role in relation to plant growth, and 2) the air conductivity at the value of P_a can be measured easily.

It is obtained from the table that the differential air conductivities range widely from 2 to 300. In the following, the relationships existing between differential air conductivity at P_a=0.2 and soil structure in the soils used will be discussed. The used soils are classfied roughly into three groups by considering both the magnitude of the differential air conductivity and the soil structure of each soil.

The first group: The soils whose differential air conductivities at P_a=0.2 are smaller than 10 belong to this group. They are Nohdai I, Nohdai II, Nohdai III, Udai I, Udai II, Udai V and Nobono II. Only

Table 3. Differential air conductivities clay contents and porosities of samples.

Kinds of soil	Soil layer		$(\Delta k_a/\Delta P_a)_{Pa=0.2}$	Clay content	Porosity
Volcanic ash soils	Nohdai	I	4	22 %	73 %
		II	2	30	75
		III	7	43	81
		IV	60	50	83
		V	80	36	79
	Udai	I	2	39	80
		II	7	41	80
		III	80	43	81
		IV	30	30	79
		V	2	13	82
		VI	30	21	79
Non-volcanic ash soils	Miedai		10	14	48
	Tsuruoka	II	300	42	70
	Shizudai	I	50	32	52
		II	10	30	48
	Nobono	II	2	37	78
		III	10	44	40

Nobono II is a non-volcanic ash soil among them. The clay contents of all soils except Udai V are high and their pore volumes are also large. These soils may be considered to be well-aggregated and consist of aggreates differing widely in size. This fact has been observed also by micro photographs for their thin layers. In other words, in each of the soils, the distribution of diameters of pores formed between the aggregates is continuous, and the pore volume as a function of pore size changes also smoothly. Consequently, the small change of P_a, ΔP_a, in the vicinity of $P_a=0.2$ does not induce the rapid change of the air-filled pore structure in each of them. Moreover, since pores formed between aggregates have a high tortuosity factor, the increase of pores available for air flow may not result in not so much increase of the air conductivity. These are the reasons why the values of $(\Delta k_a/\Delta P_a)_{Pa=0.2}$ for the soils of this group are small. In addition, the clay content of Udai V is only 13%. However, in addition to a high porosity, this soil has been also confirmed to be as well-aggregated as the other soils belonging to the first group by the observation of the micro photographs. Consequently, the small value of $(\Delta k_a/\Delta P_a)_{Pa=0.2}$ for this soil may be explained by the same reasons as those described above.

The second group: This group is characterized by the values of $(\Delta k_a/\Delta P_a)_{Pa=0.2}$ more than 10. Nohdai IV, Nohdai V, Udai II, Udai III, Udai IV and Udai VI belong to this group as volcanic ash soils. The clay contents of these soils are high and the porosities considerably large. These characteristics are similar to those of the soils classfied into the first group. However, the structures of the soils are very different from those of the soils of the first group. According to the observation of the micro photographs, the structures of the soils are massive and poor-aggregated. The pores are composed of very fine pores within large soil blocks and comparatively large pores formed between the blocks. The latter large pores are similer to fissures and their tortuosity factors are small. Consequently, the values of $(\Delta k_a/\Delta P_a)_{Pa=0.2}$ are able to become very large.

Tsuruoka II and Shizudai I belong to this group as non-valcanic ash soils. These soils have also massive and poor-aggregated structures. In addition, there exist many fissures and pores due to decayed

Table 4. Classification of soil structure based

Differential air conductivity	Typical example	
10>	Volcanic ash soils (Surface layer) Udai (240cm)	Well-aggregated Aggregated
≈10	Miedai	Poor-aggregated
>10	Volcanic ash soils (Subsoil layer) Shizudai (40cm)	Massive

roots. Shizudai II and Nobono II, Which are both subsoils of non-volcanic diluvial soils, may be also classfied into this group judging from their structures, though the values of $(\Delta k_a/\Delta P_a)_{Pa=0.2}$ are 10.

The third group: Miedai (a sandy loam) belongs to this group. A soil classfied into this group has a low clay content and is poor-aggregated. In addition, it has not large pores such as fissures. Consequently, the values of $(\Delta k_a/\Delta P_a)_{Pa=0.2}$ for soils belonging to this group may be considered to take intermediate values between those of the first group and those of the second group.

Table 4 shows a classfication of soil structures based on the values of $(\Delta k_a/\Delta P_a)_{Pa=0.2}$.

5. Tortuosities of pores available for air flow

k_a depends on both the diameters of pores availabel for air flow and the tortuosities of the pores. Here, tortuosities of pores available for air flow on the basis of a relationship between electric conductivity of soil and tortuosities of pores available for water flow will be discussed.

5-1 Experimental method

Electric conductivity of a soil was measured by packing the soil in a hollow box made of acrylic resins (2 cm×6 cm ×6 cm) in which two squares (6 cm×6 cm) of cupper polar plates are fixed 2 cm apart each other. Connecting the terminals of polar plates to an impeadance bridge (1 kc/sec), the electric resistance, R, of the soil can be measured. Then, the electric conductivity of the soil, k_e, using the following equation can be obtained.

$$k_e = C/R\ (\mho/\mathrm{cm}) \tag{7}$$

where C is the cell constant and, in this experiment, its value obtained by the standard solution of KCl was 0.166 cm^{-1}. In addition, each measured value of k_e was corrected to a value corresponding to 20°C.

Three kinds of samples whose pretreatments were different from each other were used; mixtures of clay and sand, air-dried soils and undisturbed soils. For the former two groups (samples A, B, C, D and E), not only electric conductivities as a function of degree of saturation, S_w, but also air conductivities as a function of $S_a = V_a/V_v$ (V_a=volume of air-filled pore; V_v=pore volume) were measured. On the measurements of air conductivities of the former two groups, samples packed in a glass cylinder with a 4.7 cm of inside diameter and a 15 cm of length were used, respectively.

Mixture of clay and sand: The size of the sand is 0.1~1.0 mm, and that of the clay is < 0.05 mm. The three kinds of mixture ratio (sand/clay in weight %) were adopted. Sample A consisted of only sand. For sample B, the ratio was 1.0, and it was 0.5 for sample C.

Disturbed materials: Two kinds of air-dried soil sample < 1.0 mm were used. Sample D is a paddy field soil in Udai, and sample E is an uncultivated soil in Okunakayama. Both soils are volcanic ash

on values of diffcrentiai air conductivities.

Soil structure	Characteristics of pores corresponding to $P_a=0.2$	
	Change in redius	Tortuosity
Rich in fine stable aggregates and pores between and in aggregates	Small	Large
Poor in fine stable aggregates	Middle	Middle
Composed of large soil blocks and a few large pores between blocks	Large	Small

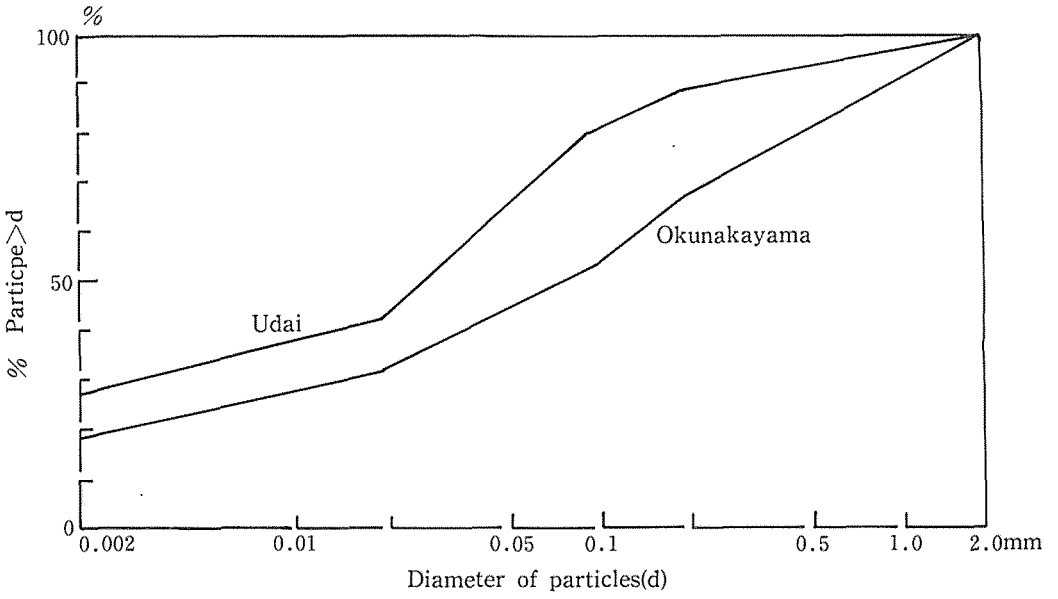

Fig. 7 Grain size accumulation curves for Udai paddy field soil and Okunakayama soil.

soils, and their grain size accumulation curves are shown in Fig. 7.

Undisturbed materials: The soil samples used were Nohdai II, Udai V, Miedai, Tsuruoka II and Nobono II.

5-2 Experimental results

5-2-1 Relationship between log k and S

The values of log k_a for samples A, B, C, D and E are shown as a function of S_a (ratio of air-filled pore volume to total pore volume) in Fig. 8, respectively. A relationship similar to those found before in Miedai, Nohdai II and Udai V (Fig. 6) is recognized in each sample. Namely, the relationship for each sample is represented by two half lines having different gradients from each other. In addition, Wyckoff and Botest[10] also have found that, in the experiment about the movement of mixed fluid of water and air passing through a porous medium, the relationship between log k_g and S_a was expressed by two straight lines as shown in Fig. 9. k_g indicates the ratio of air conductivity at a given S_a to that at $S_w=0$.

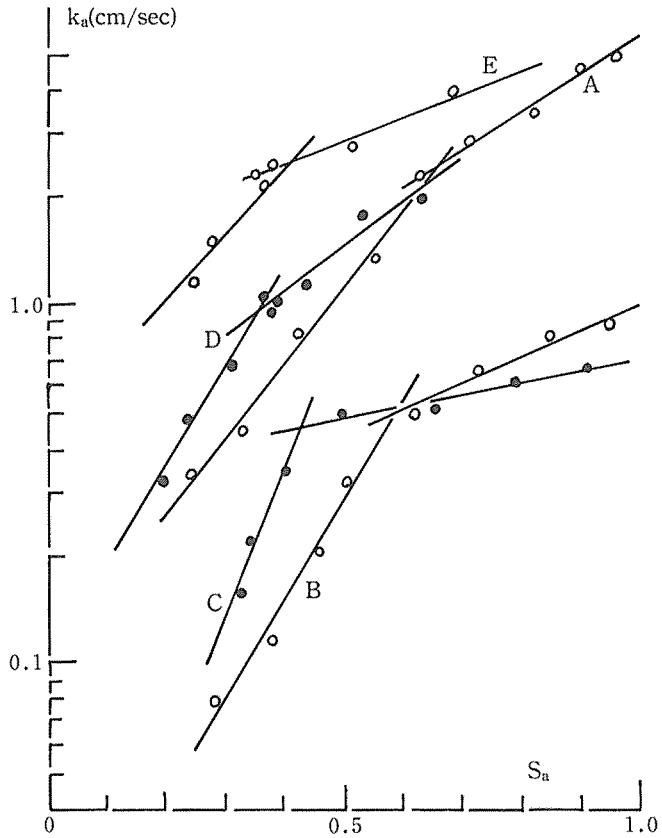

Fig. 8 Relationships between k_a and S_a for A~E samples.

5-2-2 Relationship between k_e and S_w

Several examples of the experimental results about the relationships between k_e and S_w are shown in Figs. 10 and 11. As can be read easily from the figures, the relationship for each sample is represented by a smooth S-shaped curve. Reading values of (dk_e/dS_w) from each curve, a $(dk_e/dS_w)-S_w$ curve having one maximum is obtained. As a matter of fact, the value of S_w at the maximum is equal to that of S_w at the point of inflection of each k_e-S_w curve. The values of S_w written into Figs. 10 and 11 denote those at the points of inflection of the respective k_e-S_w curves.

6. Analysis based on a capillary model

Air in a soil flows through only air-filled pores. On the other hand, electric current in a soil may be considered to flow through only water-filled pores but not through the soil solid.

Supposing that the difference in electric potential at the both ends of a soil column, whose length is L and cross sectional area is A, is E and the apparent current intensity through the soil is I, according to the Ohm's law, the following equation is obtained

$$dI = A \cdot \frac{E}{L} \cdot dk_e \tag{8}$$

Nextly, a capillary model for the above soil column, which satisfies the following assumptions will be established. 1) Each capillary in the column is continuous from an end of the column to the other end, 2)

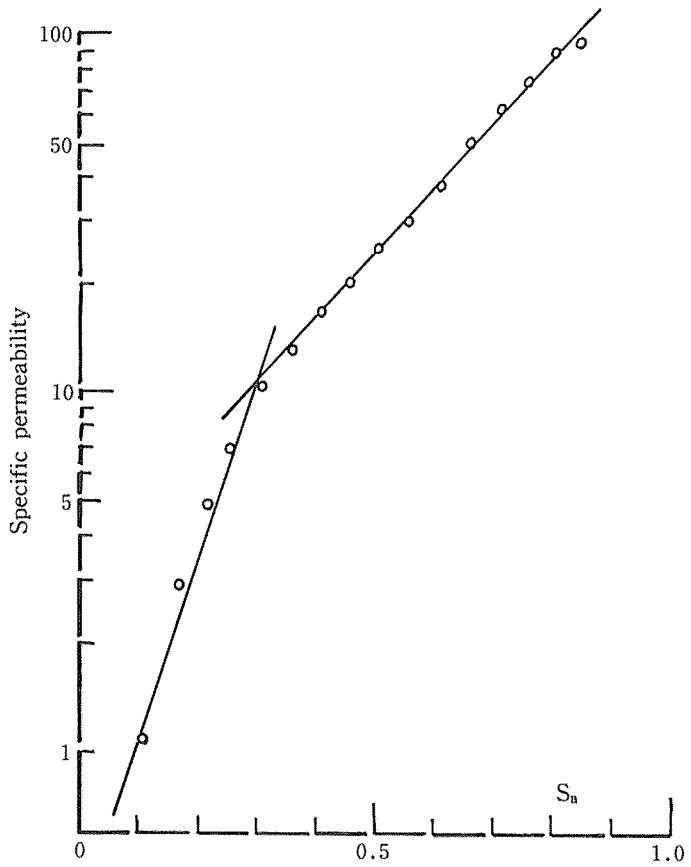

Fig. 9 Relationship between k_a and S_a (After Wyckoff and Botset).

the total number of capillaries filled with water is N and 3) the number of capillaries with a radius r_n and a length l_n in dN_n. Then, the following relation is obtained

$$N = dN_1 + dN_2 + \cdots\cdots + dN_n + \cdots\cdots$$

On the other hand, the electric current i which flows through a capillary with a radius r_n is expressed by

$$i = k_{ew} \cdot \pi r_n^2 \cdot \frac{E}{l_n} \tag{9}$$

where k_{ew} is the electric conductivity of the soil water.

Assuming that every capillary with a same radius is filled with water at a same time (a same suction), infinitesimal changes of I and S_w, dI and dS_w, induced when dN_n pieces of capillaries with a radius r_n are filled with water at a given suction are given by

$$dI = idN_n = dk_{ew} \cdot \pi r_n^2 \cdot \frac{E}{l_n} dN_n \tag{10}$$

$$dS_w = \frac{\pi r_n^2 l_n}{PAL} \cdot dN_n \tag{11}$$

where P is the porosity.

Substituting Eq. (10) into Eq.(8), the following equation is obtained

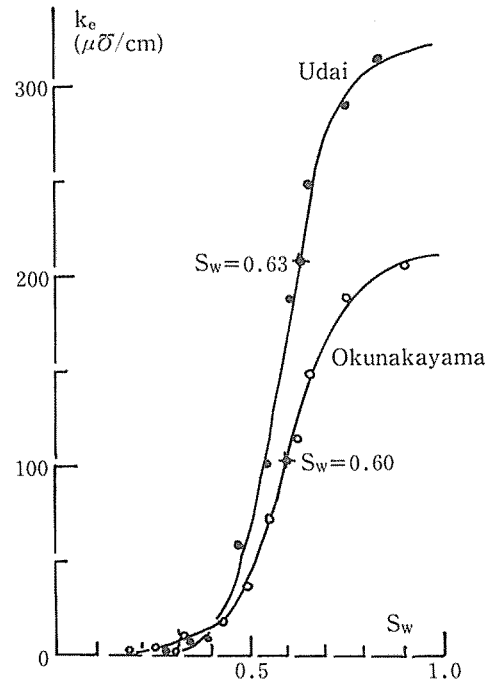

Fig. 10 Relationships between k_e and S_w for Udai and Okunakayama soils.

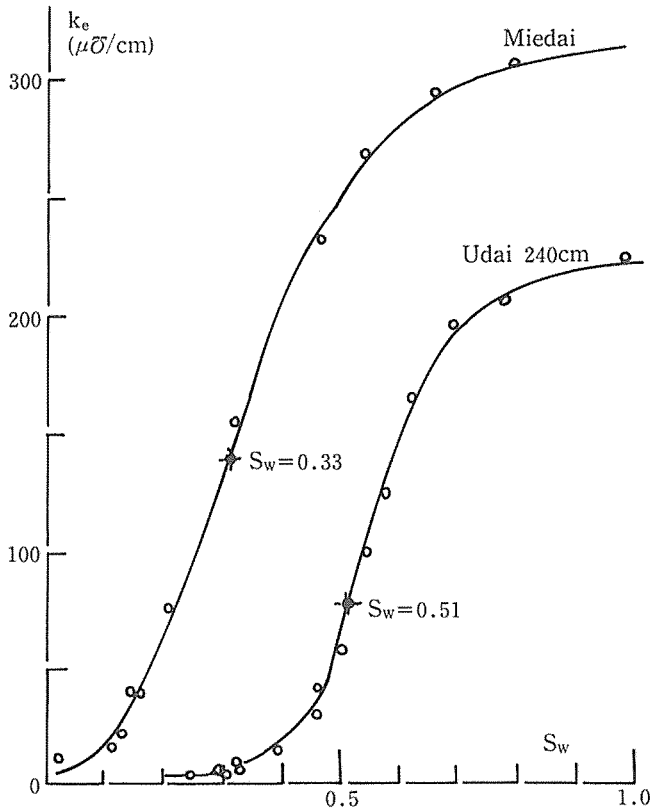

Fig. 11 Relationships between k_e and S_w for Udai and Miedai soils.

$$dk_e \frac{L}{A} \cdot k_{ew} \cdot \frac{\pi r_n^2}{l_n} \cdot dN_n \tag{12}$$

Consequently, Eq. (13) is obtained from Eqs. (11) and (12).

$$\frac{dk_e}{dS_w} = k_{ew} \cdot \frac{PL^2}{l_n^2} = \frac{C_1}{T_n^2} \tag{13}$$

where $C_1 = k_{ew} P$ and $T_n = l_n/L$. Clearly, C_1 is a constant for an identical sample, and T_n indicates the tortuosity of the capillary. Eq.(13) means that (dk_e/dS_w) is not dependent on r_n and varies inversely as only T_n^2. On the other hand, if the increment of the amount of air flow passing through a soil column, dq, depends on only the change of k_a, according to the Darcy law, the following relation is obtained

$$dq = A \cdot \frac{\Delta P}{L} \cdot dk_a \tag{14}$$

Assuming that dN_n pieces of capillaries with a radius r_n and a length ln are filled with air at a same time and applying the Hagen-Poiseuille law to the air flow in the capillaries, we obtain

$$dq = \frac{\pi r_n^4 \Delta P}{8\mu_a l_n} \cdot dN_n \tag{15}$$

where μ_a is the coefficient of viscosity of air.
According to the same procedure as that used to introduce Eq. (11), the following equation is obtained

$$dS_a = \frac{\pi r_n^2 l_n}{PAL} \cdot dN_n \tag{16}$$

where S_a is the degree of air saturation.
From Eqs. (15) and (16), Eq. (17) is gotten.

$$\frac{dk_a}{dS_a} = C_2 \frac{r_n^2}{T_n^2} \tag{17}$$

where $C_2 = P/8\mu_a$ and $T_n = ln/L$.
Eq. (17) indicates that (dk_a/dS_a) is proportional to r_n^2 and varies inversely as T_n^2. Thus, we can have (dk_e/dS_w) and (dk_a/dS_a) as a function of T_n and r_n.

7. Transition point of pores

As described before, the relationship of log k_a and S_a in a soil are represented by two half lines. Here, the intersection of the two half lines will be named "transition point of pores." Then, the equations for the two half lines are given, respectively, by

$$\begin{aligned} &(k_a)_T > k_a \quad \text{or} \quad (S_a)_T > S_a \\ &\log k_a = \alpha_1 S_a + \beta_1 \end{aligned} \tag{18}$$

$$\begin{aligned} &k_a > (k_a)_T \quad \text{or} \quad S_a > (S_a)_T \\ &\log k_a = \alpha_2 S_a + \beta_2 \end{aligned} \tag{18'}$$

where $(k_a)_T$ and $(S_a)_T$ denote the values of k_a and S_a at the transition point, respectively.

Table 5 shows the values of $(S_a)_T$ and $(S_w)_T = 1-(S_a)_T$ and the values of S_w at the points of inflection in $k_e - S_w$ curves for the samples used. From this tabel, it can be found easily in each sample, that S_w at the transition point is approximately equal to S_w at the point of inflection. In the following, the physical meaning of "transition point" based on the above fact will be discussed.

Diffentiating Eq.(18) and (18′) with respect to S, the following relation is obtained

Table 5. Values of S and S at transition point and inflection point.

Sample	Transition point of pores		Inflection point of electric conductivity
	S_a	S_w	S_w
Ⓐ Sand	0.66	0.34	0.30
Ⓑ Sand 1 : Clay 1	0.58	0.42	0.38
Ⓒ Sand 1 : Clay 2	0.43	0.57	0.41
Ⓓ Udai · air-dried	0.35	0.65	0.63
Ⓔ Okunakayama · air-dried	0.41	0.59	0.60
Nohdai (30cm)	0.44	0.56	0.64
Udai (240cm)	0.44	0.56	0.51
Miedai	0.61	0.39	0.33
Tsuruoka (40cm)	—	—	0.68
Nobono (40cm)	—	—	0.66

$$\frac{dk_a}{dS_a} = 2.30\alpha_1 k_a \qquad ((k_a)_T > k_a) \tag{19}$$

$$\frac{dk_a}{dS_a} = 2.30\alpha_2 k_a \qquad (k_a > (k_a)_T) \tag{19'}$$

Eqs. (19) and (19′) indicate that the $dk_a/dS_a \sim S_a$ curve is discontinuous at the transition point (Fig. 12). In addition, from Figs. (6) and (8) the relation $\alpha_1 > \alpha_2$ can be obtained easily.

The discontinuity of (dk_a/dS_w) at $(S_a)_T$ should be considered to be due to the discontinuity of r_n at the transition point. (dk_a/dS_a) varies proportionally as r_n^2 and inversely as T_n^2 as shown in Eq. (17). Consequently, if r_n and T_n are both continuous at the point, (dk_a/dS_a) must be not discontinuous. On

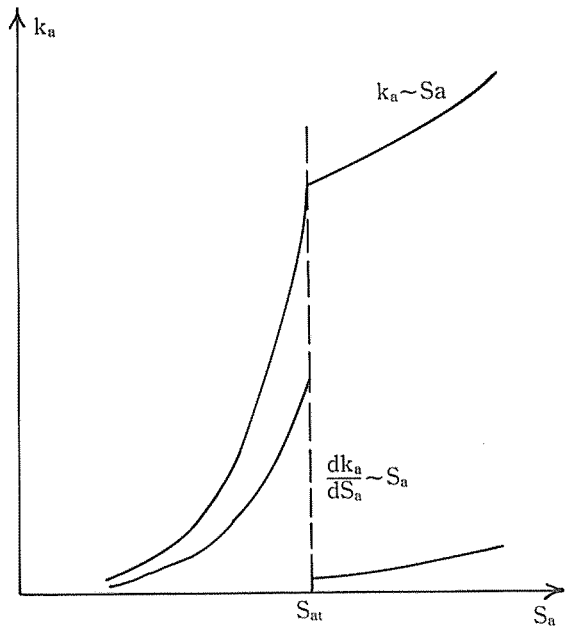

Fig. 12 Schematic representations of relationships between k_a and S_a and between (dk_a/dS_a) and S_a.

the other hand, the discontinuity of (dk_e/dS_w) at $(S_w)_T$ is not found in each k_e-S_w curve in Fig. 11, while (dk_e/dS_w) is in inverse proportion to T_n^2 indicated in Eq. (13). This means that T_n changes continuously at $(S_w)_T$. Therefore, r_n has to be discontinuous at the transition point. In other words, though the value of r_n decreases gradually as S_a increases except the vicinity of the transition point, r_n decreases discontinuously with slight increase of S_a in the vicinity of the transition point.

Nextly, S_a will be divided into two regions-Region $(r^{(1)}, T^{(1)})$ where $(S_a)_T > S_a$ and Region $(r^{(2)}, T^{(2)})$ where $S_a > (S_a)_T$—, and characteristics are considered in changes of T_n and r_n/T_n with S_a in the respective regions. Region $(r^{(1)}, T^{(1)})$: As a matter of fact, $r^{(1)}$ decreases as S_a increases. Namely, $r_n^{(1)} > r_{n+1}^{(1)} > r_{n+2}^{(1)}$. Generally, the number of large pores is less than that of small pores. Therefor, a large capillary which is formed by connection of many large pores may be considered to be very twisty. This means that the larger $r^{(1)}$ is, the larger $T^{(1)}$ becomes. That is, $T_n^{(1)} > T_{n+1}^{(1)} > T_{n+2}^{(1)}$. This inclination coincides with the conclusion obtained from Eq. (13) and Figs. (10) and (11). According to Eq. (19), the value of (dk_a/dS_a) increase with S_a since k_a increases with S_a. This indicates that $(r_n/T_n)^2$ in Eq. (17) increases with S_a. Namely,

$$\frac{r_n^{(1)}}{T_n^{(1)}} < \frac{r_{n+1}^{(1)}}{T_{n+1}^{(1)}} < \frac{r_{n+2}^{(1)}}{T_{n+2}^{(1)}}.$$

As described before, (dk_a/dS_a) becomes discontinuous at $S_a=(S_a)_T$ (the transition point) because of the discontinuity of r_n. After crossing the transition point, (dk_a/dS_a) is expressed by Eq.(19′). As stated before, α_2 is Eq. (19′) is smaller than α_1 in Eq. (19). On the contrary, (dk_e/dS_w) is continous at $S_a=(S_a)_T$ as shown in Fig. 13. Since (dk_e/dS_w) shows the maximum value at the point, the tortuosity of capillary as path of water, T_n, becomes the minimum value near the point as understood easily from Eq. (13). Region $(r^{(2)}, T^{(2)})$: $r^{(2)}$ clearly decreases with S_a in the same manner as in Region $r_n^{(2)} > r_{n+1}^{(2)} > r_{n+2}^{(2)}$. According to Eq. (19′), the value of (dk_a/dS_a) increases with S_a. Consequently, considering Eq. (17), we obtain that

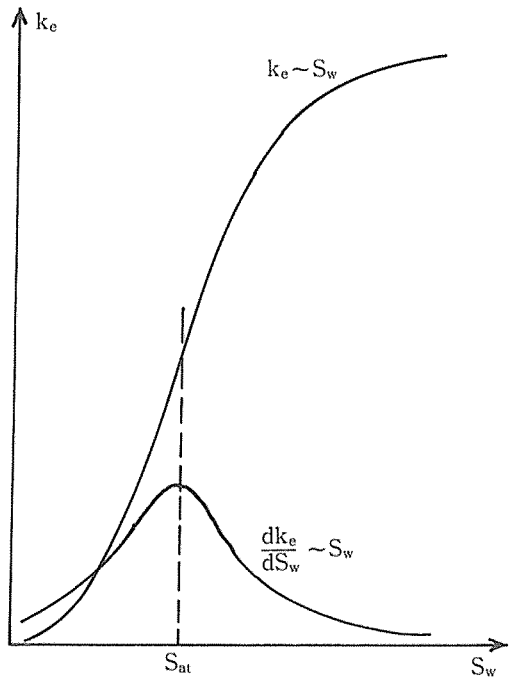

Fig. 13 Schematic representations of relationships between k_e and S_w and between (dk_e/dS_w) and S_w.

$$T_n^{(2)} > T_{n+1}^{(2)} > T_{n+2}^{(2)} \text{ and } \frac{r_n^{(2)}}{T_n^{(2)}} < \frac{r_{n+1}^{(2)}}{T_{n+1}^{(2)}} < \frac{r_{n+2}^{(2)}}{T_{n+2}^{(2)}}.$$

However, since $\alpha_1 > \alpha_2$, the degree of increase of $(r_n^{(2)}/T_n^{(2)})$ is smaller than that of $(r_n^{(1)}/T_n^{(1)})$. On the other hand, as described before, the tortuosity of capillary as path of water shows the minimum value at the transition point, and, after that, it increases with S_a (refer to Eq. (13) and Fig. (13)). This may be due to a fact that electric current has to flow through a roundabout path because water-filled pores are scattered in Region $(r^{(2)}, T^{(2)})$.

The characteristics in changes of T_n and r_n/T_n with S_a described above are not infered on the basis of enough experimental results. Further studies are needed.

8. Estimation of amount of immobile water

8-1 Introduction

It has been known well that the Darcy law is valid for flow of fluid such as air and water. However, even when water flows through a saturated soil, all of water in the pore does not take part in the flow. Bydagoffskii[2] has pointed out that a part of water in soil pores is immobile and the amount of immobile water should be substracted from the total amount of the pores on the calculation of water permeability. Rode[7] also has emphasized that there are pores occupied by inactive water in a clayey soil. Though the existence of immobile water, which can not take part in saturated water flow, has been recognized widely, a method to determine the amount of immobile water has not yet been established.

In this capter, the author will propose a method to estimate the amount of the immobile water based on an analogy between soil pore structure governing water flow and that governing air flow, and discuss some physical properties of immobile water on the basis of results obtained using the proposed method.

8-2 Theoretial consideration

Many researches about factors determining the conductivity of a fluid flow through a porous medium such as hydraulic conductivity and air conductivity have been performed in the past. Zunker has introduced the following equation expressing hydraulic conductivity of a soil, k_w.

$$k_w = \frac{C}{\mu_w U^2}\left(\frac{P_{ol}}{1-P}\right)^2 \tag{20}$$

where C is the coefficient related to the shape of soil particles, μ_w is the coefficient of viscosity of water, U is the specific surface area of soil particles, P_{ol} is the effective porosity for water flow, and P is the total porosity.

According to the Kozeny-Carman equation, k_w is given by

$$k_w = \frac{1}{k_0 \mu_w U^2 T} \cdot \frac{P^3}{(1-P)^2} \tag{21}$$

where k_0 is the coefficient related to the shape of the capillaries, and T is the tortuosity of the capillaries.

Bydagoffskii also has proposed the following equation

$$k_w = \frac{\alpha_0 (P - W_H)^3}{U^2} \tag{22}$$

where α_0 is the constant, and W_H is the amount of inactive water.

In all the above equations, k_w is expressed as a function of P. On the other hand, as described before, k_a is given as a function of P_a as shown in Eq.(5). Consequently, it may be reasonable to consider that P or P_a is the most important factor detemining water flow or air flow. However, there seems to be a great difference between P for water flow and P_a for air flow. Since immobile water exists certainly for water

flow as seen in Eqs. (20) and (22), P can not be used as an exact index of pores which water passes through. On the contrary, because the existence o f immobile air may be not considered, P_a seems to be used as an exact index of pores which air flows through. Paying attention to the difference, a method to evaluate the amount of immobile water on the basis of the following assumptions is introduced: 1) The factors defining k_w such as U and C found in the above equations except P and μ_w are quite same to those defining k_a. That is, the conductivity of any fluid flowing through a porous medium is determined by only the coefficient of viscosity of the fluid, μ, and the ratio of pore volume available for the saturated fluid flow to the total volume of the medium, P_m. 2) As stated before, all of air-filled pores is available for air flow. In other words, air in the porous medium is all mobile.

Intrinsic perpeability, K[3], is given by

$$K = \frac{k\mu}{\rho_w g} \quad \text{(darcy)} \tag{23}$$

where ρ_w is the density of water, and g is the acceleration of gravity. The word of darcy shown in the parenthesis denotes an unit of K. When the amount of flow is 1 cm²/sec under a condition where the pressure gradient is 1 atm/cm², the cross-sectional area of the medium is 1 cm² and the coefficient of viscosity of fluid is 0.01 poise, K becomes equal to 1.0 darcy.

As being well known, K is defined only by the pore structure of a porous medium. Namely, it is not dependent on kinds of fluid. If a porous medium has not immobile water under the saturated water condition, P is equal to P_m, and P is also equal to P_a at $S_w=0$. Therefore, the following relation can be expected

$$K_a(\text{at } S_w=0) = K_w(\text{at } S_w=1) \quad \text{(darcy)} \tag{24}$$

where K_a and K_w are intrinsic permeabilities for air and water, respectively. The validity of Eq.(24) has been confirmed using porous media having inactive particle surfaces (having not immobile water) such as a sandstone. Table 6 shows the results obtained by Muskat[5]. The agreement of K_a and K_w is very good.

Table 6. Intrinsic permeabiiities of sands and sandstones.

Samples	Intrinsic permeability (darcys)	
	K_a	K_l
40～45 mesh sand	139.13	139.40 (H_2O)
80～100 mesh sand	24.90	22.00 (H_2O)
No.1 sandstone(Woodbime)	1.18	1.20 (CCl_4)
No.2 sandstone(Woodbine)	1.56	1.57 (H_2O)
No.3 sandstone(Woodbine)	1.63	1.63 (H_2O)
No.4 sandstone(Berea)	1.54	1.50 (H_2O)

However, as, in a case of soil, immobile water exists in the pores, the total porosity, P, is larger than P_m. This means that K_a at $S_w=0$ is larger than K_w at $S_w=1$. That is, P_a becomes equal to P_m at a given degree of saturation, $(S_w)_{P_a=P_m}>0$. Then, the following relation may be expected

$$K_a(\text{at } (S_w)_{P_a=P_m}) = K_w(\text{at } S_w=1)$$

Inversely, if the value of S_w where $K_a=K_w$ at $S_w=1$, can be found it will be expected that the value is approximately equal to the amount of immobile water. This is the principle of the method proposed here to estimate the amount of immobile water.

8-3 Experimental method and results

8-3-1 Measuring methods

The measurement of air conductivity, K_a, as a function of $P_a(S_a)$ was done using the same aparatus and by the same procedure described in Chapter 2. Saturated hydraulic conductivities, k_w, were measured using a constant head permeameter. Sample tubes of glass with a 4.7 cm of inside diameter and a 15 cm of length were used for sands and disturbed soils, and those of brass with a 4.8 cm of inside diameter and a 15 cm of length were used for undisturbed soils. Before measuring k_w, each sample was saturaded with deaired water under a reduced pressure. After measuring k_w, k_a was measured as a function of P_a. The values of K_a and K_w were calculated from the measured values of k_a and k_w using Eq. (23). The water characteristic curve of each sample was obtained by using a suction plate method ($<$pF2.0) and a centrifugal method ($>$pF2.0).

8-3-2 Materials

Sands: 2~1 mm, 1~0.5 mm and 0.5~0.25 mm

Disturbed soils: Udai paddy field soil, and Okunakayama uncultivated subsoil. Both soils were air-dried and sifted through a screen with a 1.0 mm of hole.

Undisturbed soils: 17 soils used in the previous experiment.

8-3-3 Results

The results for the sands are shown in Table 7. K_a in the table means K_a at $S_w=0$. In each sample, the value of K_a agrees well with that of K_w. This fact indicates that there does not exist immobile water in each sand. That is, it can be regarded that $P=P_m$ in sands. Table 8 shows the results for the disturbed soils.

Fig. 15 is a schematic representation of immobile water. It can be recognized from the table that K_a becomes equal to K_w at a considerably high value of S_w (57% and 65%). I n other words, the amount of immobile water in the each soil can be regarded to be considerably large. In addition, the pF values correspondig to the amounts of immobile water for Udai soil and Okunakayama soil are 1.9 and 1.6, respectively. The results for the undisturbed soils are represented in Table 9. It can be read also from the table that most of soils has a considrable amounst of immobile water. The average amount of immobile water for the valcanic ash soils except Udai V is 55 % in volume basis and 68% in degree of saturation. The pF value corresponding to the S_w is 3.0. On the other hand, the average amount of immobile water for the non-volcanic ash soils except Miedai (Sandy soil) is 39 % in volume basis and 64% in dedegree of saturation. The pF value corresponding to the S_w is 2.6.

Table 7. Intrinsic permeabilities of sands (darcys).

Sample	K_a	K_w
2~1mm	$9.5^{\times 10^2}$	$9.2^{\times 10^2}$
1~0.5mm	5.6	5.7
0.5~0.25mm	2.5	2.5

Table 8. Amounts of immobile water in air-dried disturbed soils.

Sample	K_w (darcys)	P_a corresponding to $K_a=K_w$	Water content (volume basis)	Degree of saturation	Water content (weight basis)
Udai	2.2	33 %	43 %	57 %	69 %
Okunakayama	3.9	27	49	65	81

Table 9. Amounts of immobile water in undisturbed samples.

Kinds of soil	Soil layer	Sampling depth	K_w (darcys)	P_a corresponding to $K_a = K_w$	Water content (volume basis)	Degree of saturation	Water content (weight basis)	pF
Volcanic ash soils	Nohdai I	0～ 10 cm	2.0	30 %	43 %	56 %	62 %	2.9
	Nohdai II	30～ 40	2.1	38	37	50	61	3.0
	Nohdai III	43～ 53	3.5	28	52	65	100	3.2
	Nohdai IV	80～ 90	7.6	21	62	74	133	3.4
	Nohdai V	140～150	21	27	57	72	130	3.1
	Udai I	15～ 25	5.3	41	36	47	59	3.2
	Udai II	100～110	1.6	12	67	85	115	3.0
	Udai III	150～160	5.2	21	60	74	113	3.0
	Udai IV	180～190	2.5	17	62	79	109	2.6
	Udai V	240～250	2.1	80	0	0	165	2.0
	Udai VI	300～310	2.0	18	64	79	120	2.7
Non-volcanic ash soils	Miedai	15～ 25	7.1	42	4	9	4	2.2
	Tsuruoka II	40～ 50	0.20	2	60	89	79	3.2
	Shizudai I	5～ 15	3.2	16	34	68	28	1.9
	Shizudai II	40～ 50	5.8	30	18	37	30	2.2
	Nobono II	40～ 50	4.4	36	41	53	70	3.0
	Nobono III	65～ 75	0.29	15	42	74	37	2.5

8-4 Discussion

(1) The values of S_w at the inflection points and the transition points, and the amount of immobile water for the typical seven soils among the soils used are shown in Table 10. The facts read from the table are: 1) The three values of S_w in each volcanic ash soil except a sandy one (Udai) take a same value approximately, respectively. 2) In each non-volcanic ash soil except a sandy one (Miedai) the value of S_w at the inflection point is roughly equal to the amount of immobile water. 3) In sandy soils, since the amounts of immobile water are vary small, the values of S_w at the inflection points and the transition points do not coincide with the amount of immobile water.

The above facts suggest that 1) in the soils except the sandy soils, water in pores drained in Region ($r^{(1)}$, $T^{(1)}$) is mobile and water held by pores in Region ($r^{(2)}$, $T^{(2)}$) is immobile because the radii of the pores are very small and the water in the pores has a strong interaction with the soil particles, and 2) since, in the sandy soils, the clay contents are very low and the numbers of pores with very small radii are a few, the amounts of immobile water may become extremely low.

(2) As described in the previous clause, both the average amount of immobile water and the pF value corresponding to it in the volcanic ash soils are larger than those in the non-volcanic ash soils, respectively. This fact may be considered to reflect the structural characteristics of the volcanic ash soils. In addition, the pF value corresponding to the average amount of immobile water coincides with that corresponding to the moisture content of rupture of capillary bond of Kanto loam obtained by Shiina[9]. The moisture content of rupture of capillary bond indicates the water content when water in capillaries in a soil become discontinuous each other. This concept has been proposed by Rode. Rode has showed that water existing below the water content is poor in mobility and difficult to move in the liquid state. Consequently, it may be considered that the amounts of immobile water in the volcanic ash aoils obtained here are corresponding to the moisture contents of rupture of capillary bond in the respective soils.

In order to obtain more detailed and more physical knowldges about the structural characteristics of volcanic ash soils, further studies are needed.

9. Conclusions

The following conclutions were obtained from the measured values of air conductivities, k_a, as a function of the ratio of air volume to the total pore volume, P_a, in various soils.

(1) The Darcy law was valid for not only water flow but also air flow in soil.

(2) The relationship between log k_a and P_a in each soil was expressed by two half lines with different gradients from each other.

(3) The differential air conductivity obtained by differentiating k_a with respect to P_a in a soil is a physical quantity reflecting the soil structure. It can be used as a good index classifying the soil structure.

(4) The intersection of the two half lines in the log k_a~P_a relationship of a soil was named "transition point of pores." In most of soils used, the values of degree of saturation, S_w, at the transition points were approximately equal to those at the inflection points in respective S_w~ electric conductivity curves. The physical meaning of "transition point" was clarified using a capillary model. That is, the magnitude of radius of capillary pores available for air flow becomes greatly discontinuous at the transition point.

(5) The amounts of immobile water in all the soils used were obtained by measuring the respective air and water intrinsic permeabilities. The pF values corresponding to the average amounts of immobile water for the volcanic ash soils and the non-volcanic ash solis are 3.0 and 2.6, repectively.

References

1) BUCKINGHAM, E.; Contribution to our knowledge of the aeration of soils, U. S. Soils Bull. 25, 1904.

2) BYDAGOFFSKII, A. E.; Water infiltration into soil, Kenkyu no Shiryou to Kiroku, No. 9, p. 20, 1959.
3) KRIMENTOFF, P. P.; Dynamics of Ground Water, p. 29, Moscow, 1961.
4) LINDQUIST, E.; On the flow of water through porous soil, Report of 1st Cong. Large Dams, p. 181, 1933.
5) MUSKAT, M.; The flow of homogeneous fluids through porous media, p. 93, J. W. Edwards, Inc., Michigan, 1946.
6) NAGATA, N.; Mesurement of air permeability of soil, Guidbook on damage by blight and harmful insects in soil, pp. 67～77, Nihon Shokubutsu Boekikyokai, 1967.
7) RODE, A. A.; Soil Water, p. 56, Moscow, 1955.
8) RODE, A. A.; Soil Water, p. 95, Moscow, 1955.
9) SHIINA, K.; Studies on mechanism of reduction of content in upland fields, Bull. Nat. Res. Inst. Agr. Eng., No. 1, p. 110, 1963.
10) WYCKOFF, R. D. and BOTSET, H. G.; The flow of gas-liquid mixtures through uncosolidated sands, Pysics Vol. 7, p. 325, 1936.

摘　　要

自然構造土壌の通気性について

長　田　　昇

土壌の構造を乱さない採土試料について通気性の特性を研究した。充塡試料との比較において，また透水性と比較しながら，さらに通気間ゲキの屈曲度を電気伝導度によって考察しながら，通気間ゲキの特性を次のようにまとめることができた。

まず，土壌の通気性は透水性と同じように，ある圧力勾配の範囲内では Darcy 法則が適用でき，通気係数によって通気性を評価できることが実験的に確認された。また，空気間ゲキ率と通気係数の間にはそのままでは一定の関係が認め難いが，これは採土試料の状態では間ゲキ内に大気に開放されていない空気間ゲキが残されているためと考えられる。そこで，水で試料を飽和した後排水しながら開放状態をつくり，排水過程で空気間ゲキ率と通気係数の関係を求めた。その結果，それらの間には一定の指数曲線で表わされるような相関関係が認められた。

さらに，通気間ゲキの増加に伴なう通気性増加の傾向を示すと考えられる通気性増大係数を採土試料によって求め分類した。その値の大小によって土壌構造が判別され，自然構造土壌の構造性が分類されることが分かった。とくに，火山性土壌の表土と心土の構造の相異や粘土質土壌と砂質土壌の構成材料の粒度による構造の相異などが団粒構造の指標として明らかにされた。

その上，通気間ゲキには通気性が極端に変化する特異点が認められ，その特異点（通気間ゲキの変異点）を境界として，開放毛管とその屈曲度の性質が質的に変化することが毛管モデルによって考察された。しかも，その特異点は火山性土壌でほぼ pF 3.0，非火山性土壌でほぼ pF 2.6 に相当する毛管径の付近であると考えられる。通気間ゲキと透水間ゲキの相等性の上に立って，自然構造の透水時難流動水分量を計算した結果では，ほぼ特異点に相当する水分量であることが明らかにされ，通気間ゲキの変異点に相当する毛管径では土壌の透過間ゲキ特性が大きく変化するのであろうと結論づけられた。

このように，通気性について Darcy 法則を適用して，通気係数で評価することによって，自然構造を乱さない土壌試料の間ゲキ構造の指標とその変化の特性を明らかにすることができた。